

Kinetics of surface growth with coupled diffusion and the emergence of a universal growth path

Rami Abi-Akl^a, Rohan Abeyaratne^a, Tal Cohen^{a,b,*}

^a*Department of Mechanical Engineering, Massachusetts Institute of Technology, 77 Massachusetts Avenue
Cambridge, Massachusetts, 02139, USA*

^b*Department of Civil & Environmental Engineering, Massachusetts Institute of Technology, 77
Massachusetts Avenue Cambridge, Massachusetts, 02139, USA*

Abstract

Surface growth, by association or dissociation of material on the boundaries of a body, is ubiquitous in both natural and engineering systems. It is the fundamental mechanism by which biological materials grow, starting from the level of a single cell, and is increasingly applied in engineering processes for fabrication and self-assembly. A significant complexity in describing the kinetics of such processes arises due to their inherent coupled interaction with the diffusing constituents that are needed to sustain the growth, and the influence of local stresses on the growth rates. Moreover, changes in concentration of solvent within the bulk of the body, generated by diffusion, can affect volumetric changes, thus leading to an additional interacting growth mechanism. In this paper we present a general theoretical framework that captures these complexities to describe the kinetics of surface growth while accounting for coupled diffusion. Then, by combination of analytical and numerical tools, applied to a simple growth geometry, we show that the evolution of such growth processes rapidly tends towards a universal path that is independent of initial conditions. This path, on which surface growth mechanisms and diffusion act harmoniously, can be extended to analytically portray the evolution of a body from inception up to a treading state, in which addition and removal of material are balanced.

Keywords: Surface growth, driving force, universal path

1. Introduction

Material growth is seldom governed by a single growth mechanism, but is rather a result of an interplay between several mechanisms that act in concert. Even in the simplest conceivable growth settings, such as 3D printing, formation of a body is often highly dependent upon chemo-mechanically coupled processes that occur within the material and can lead, for example, to shrinkage and residual stresses (Gibson et al., 2014; Correa et al., 2015; Szost et al., 2016; Bauhofer et al., 2017; Zurlo and Truskinovsky, 2017). While 3D printing serves as an example fabrication technique in which material is sequentially added on the boundaries of a body, other engineered processes may occur spontaneously, as in chemical deposition (Kaur et al., 1980; Nair and Nair, 1991; Mane and Lokhande, 2000; Mattevi et al.,

*Corresponding author: talco@mit.edu

2011), and growth of nanotube forests (Meyyappan et al., 2003; Kim et al., 2003; Louchev et al., 2003). Such *surface growth* mechanisms, are also ubiquitous in nature and are imperative for maintaining life. The cytoskeleton of animal cells grows by polymerization of actin gel on the inner side of the cell membrane¹, a surface growth process that is responsible for cell motility (Mitchison and Cramer, 1996; Mogilner and Oster, 1996); tissue level growth and remodeling of biological systems also involves material deposition and removal on a surface (Ateshian, 2007) as for example, the renewal cycle of skin creating cell layers at the bottom surface of the hypodermis (Tepole et al., 2011; Zöllner et al., 2012); seashells grow by deposition of material on an external surface (Thompson, 1970; Skalak et al., 1997; Moulton et al., 2012; Goriely, 2017); and tree trunks grow by addition of layers underneath the bark (Archer, 2013). In all of these examples, the grown body, although generated on a surface, can simultaneously evolve by chemo-mechanical processes occurring in the bulk that can, in-turn, influence the surface growth reaction. Eventually, the interplay between these mechanisms is what determines the evolution of the growing body and is thus the focus of the present study.

To consistently capture the complexities that arise due to the existence of multiple reacting species in an open system, the present approach deviates from the more familiar *kinematic growth theories* (Ambrosi and Mollica, 2002; Ben Amar and Goriely, 2005; Ambrosi and Preziosi, 2009; Ben Amar and Ciarletta, 2010; Ambrosi et al., 2011; Dervaux and Ben Amar, 2011; Menzel and Kuhl, 2012; Humphrey et al., 2014; Cyron and Humphrey, 2017) and attempts to represent the growth response by employing a thermodynamically consistent *kinetic theory*. This is achieved by building on recent constitutive models for polymers that account for both large deformations and fluid diffusion (Fried and Gurtin, 2004; Hong et al., 2008; Duda et al., 2010; Chester and Anand, 2010; Loeffel and Anand, 2011). Surface growth is then accounted for by permitting a chemical reaction between the two species (i.e. a solid matrix, and a permeating solvent), on the boundaries of the body. In general, we consider a solid matrix permeated by a solution that contains units that can associate to (or dissociate from) the body. The solution can diffuse within the solid matrix and the resulting body can grow by a combination of two mechanisms, namely swelling and surface growth. Ultimately, we seek to understand the evolution of such a system, and to determine under what conditions the body evolves towards a steady-state in which addition and removal of solid material are balanced, also called treadmilling.

Although some available studies model surface growth by considering a localized zone of volumetric growth (DiCarlo, 2005; Ciarletta et al., 2013; Holland et al., 2013; Papastavrou et al., 2013), thus facilitating the use of kinematic growth theories, in the present study we distinguish between surface growth and volume growth. This dissimilarity has been emphasized by Skalak et al. (1997) and later illustrated by Menzel and Kuhl (2012) and is primarily due to the absence of a conventional natural global reference configuration in the case of surface growth, as manifested by the addition and removal of material points on the boundaries of the body and the resulting accumulation of residual stresses. The

¹Actin gel is a fundamental building block of the cytoskeleton of mobile animal cells. It composes both the lamellipodium at the leading edge and the cell cortex and is the major engine of cell movement. Persistent polymerization of actin pushes against the cell membrane creating motion of the entire cell in a process which is controlled by the concentration of actin monomers.

absence of a global natural reference configuration limits the application of usual continuum representations of the solid body, and probably explains the focus on kinematics in available studies of surface growth (Skalak et al., 1982, 1997; Menzel and Kuhl, 2012; Moulton et al., 2012). Recent studies (Tomassetti et al., 2016; Sozio and Yavari, 2017; Ganghoffer and Goda, 2018) have explored new ways to examine surface growth. Specifically, Tomassetti et al. (2016) identified that for the particular surface growth scenario considered therein, the grown body possesses a natural global reference configuration if relaxed into a four-dimensional space. Building on this notion and extending it to an arbitrary surface growth geometry, in the next section we begin by defining the kinematic representation of the growth problem. Then in section 3 we apply the usual tools of continuum mechanics to formulate the governing equations of mass conservation and mechanical equilibrium by alternating between current and reference configurations to provide a measure for elastic deformation and stresses with respect to a stress-free state. In section 4, the definition of a natural reference configuration facilitates a thermodynamically consistent derivation of configurational forces that drive association and dissociation. By examining those driving forces it will be shown that the growth reaction is coupled to particle diffusion, species concentrations, and internal stresses within the body. The theoretical framework is summarized in section 5, where a specific set of constitutive equations is provided to represent the growth of polymer gels. By applying these constitutive relations, the general theoretical framework is specialized to a simple growth geometry in section 6. It is shown that the evolution of such coupled growth processes rapidly tends towards a *universal path* that is independent of initial conditions. Along this path the different growth mechanisms, i.e. swelling and surface growth, act harmoniously.

2. Problem setting and kinematic representation

Consider a non-dilute solution of solvent units. Now, introduce into that solution an object of arbitrary shape that by chemical reaction on its surface promotes association of solvent units to form a solid matrix. That matrix can in-turn mix with the solvent and swell to form an aggregate body composed of both a solid matrix and an impregnating solvent. Since the binding reaction can occur only on the growth surface, where it is energetically favorable, the previously formed layers are constantly pushed away from the growth surface as new layers are formed. This process may thus induce a build-up of internal stresses which can lead to subsequent dissociation. Additionally, a continuous supply of solvent units is required at the growth surface to sustain the growth and to occupy the body region, implying that the growth reaction is intimately coupled with the diffusion process.²

As the growth progresses, both the region $\mathcal{R}(t)$ occupied by the body in the *physical space* and the image region $\mathcal{R}^R(t)$ in the *reference space* continuously evolve due to the reorganization of constituents (Fig. 1). Nevertheless, though the region $\mathcal{R}^R(t)$ is evolving, each material point sustains its location in the reference space, as long as it is attached to the body. As a convention, the superscripted ‘R’ denotes values in the reference frame.

²A comprehensive nomenclature can be found in Appendix A.

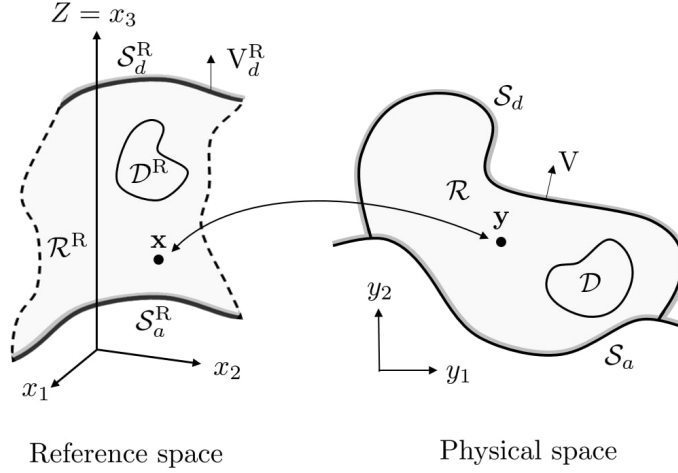


Figure 1: Schematic of the grown body in its reference and current ($\mathcal{R}^R, \mathcal{R}$) configurations, respectively, and the corresponding association ($\mathcal{S}_a^R, \mathcal{S}_a$) and dissociation ($\mathcal{S}_d^R, \mathcal{S}_d$) surfaces. An arbitrary material subregion with its counterpart in the current frame ($\mathcal{D}^R, \mathcal{D}$) is also shown as well as the boundary velocities in the reference and current frame, (\mathbf{V}^R, \mathbf{V}), respectively. For illustration purposes, the grown body is represented here in a 2D physical space and its reference configuration is embedded in a 3D space.

Physical space. In the physical space we represent the true, current configuration of the problem. A spatial point \mathbf{y} is described by a set of orthonormal coordinates (y_1, y_2, y_3) . The region $\mathcal{R}(t)$ occupied by the body in its current configuration at time t is referred to as the body manifold; $\partial\mathcal{R}(t)$ denotes the surface boundary of the body manifold which can alternatively be written as $\partial\mathcal{R}(t) = \mathcal{S}_a(t) \cup \mathcal{S}_d(t)$, where $\mathcal{S}_a(t)$ and $\mathcal{S}_d(t)$ represent the association and dissociation surfaces respectively in the physical space at time t . To relate between a volume element in its reference and current configurations it is useful to define an arbitrary material subregion $\mathcal{D}(t)$ which is associated with a constant group of material points though solvent may diffuse in and out of it.³

Reference space. In the reference space, the material manifold $\mathcal{R}^R(t)$ represents the solid matrix in a stress-free and dry state (i.e. without any solvent) and a material point \mathbf{x} is described by a set of orthonormal coordinates (x_i) , with $i = 1 \dots n+1$, where $n+1$ denotes the dimension of the reference space. Notice that the material manifold (including its boundary surface $\partial\mathcal{R}^R(t)$ and the pre-image of $\mathcal{D}(t)$ that is denoted by $\mathcal{D}^R(t)$) is time dependent. This is a direct result of the association and dissociation on the boundaries.

In the above discussion we have taken the existence of a reference configuration for granted. However, since the solid medium is continuously evolving, with material particles being added and removed from the body, and with accumulation of residual stresses, it is not a straightforward task to find an unambiguous global natural reference configuration. Nevertheless, it is imperative to define the stress-free configuration at every point, in order to

³A smooth transition from association to dissociation can be facilitated by the definition of the kinetics of growth to avoid singularities at the intersection between \mathcal{S}_a and \mathcal{S}_d . The specific discussion on singular solutions is beyond the scope of this work.

evaluate the stress field in the growing material. To that end, a natural, geometrically defined, reference configuration is essential. Though in the physical space such a configuration does not necessarily exist, under certain conditions, it is possible to define a stress-free reference configuration in a higher-dimensional space, as demonstrated by Tomassetti et al. (2016), for the specific example of spherical growth. Such a transformation can exist if (i) the growth is continuous in time (i.e. addition of solid volume over time constitutes a continuous function), and (ii) the reference metric of the infinitesimally thin (2D) layer, formed on the growth surface at a given time, can be isometrically embedded with finite bending in \mathbb{R}^n with $n \geq 3$. Hence, in the reference space, the grown layers are hyper-surfaces and can be, intuitively, stacked on top of one another in a chronological order along the $n+1$ dimension, to comprise the isometric embedding of the entire body in \mathbb{R}^{n+1} . More specifically, if the embedding of the 2D grown layer in the reference space is defined by $\mathcal{S}_a^R(t) \subset \mathbb{R}^n$, then the material manifold in the reference space is chosen as the Cartesian product

$$\mathcal{R}^R(t) = \mathcal{S}_a^R(t) \times Z(t), \quad (1)$$

where $Z(t) = [Z_a, Z_d]$ is the interval along the $n+1$ dimension, with Z_a and Z_d denoting the coordinate along the $n+1$ dimension of the association and dissociation surfaces respectively, and $\mathcal{R}^R(t) \subset \mathbb{R}^{n+1}$. A wide group of problems can be limited to *simple growth surfaces* which we define here as growth surfaces that generate 2D layers that possess a stress-free reference configuration in \mathbb{R}^3 .

Having established that a global natural reference configuration of a body grown by the local mechanism of surface growth can be defined, we proceed by employing such a transformation in a general sense. Hence we define the mapping of a material point \mathbf{x} in the reference space into a spatial point \mathbf{y} in the physical space by the time dependent transformation

$$\mathbf{y} = \hat{\mathbf{y}}(\mathbf{x}, t), \quad \mathbf{x} \in \mathcal{R}^R(t), \quad \mathbf{y} \in \mathcal{R}(t). \quad (2)$$

The particle velocity and the deformation gradient tensor are respectively defined by

$$\mathbf{v}(\mathbf{x}, t) = \frac{\partial \hat{\mathbf{y}}(\mathbf{x}, t)}{\partial t}, \quad \mathbf{F}(\mathbf{x}, t) = \frac{\partial \hat{\mathbf{y}}(\mathbf{x}, t)}{\partial \mathbf{x}}, \quad (3)$$

and

$$J(\mathbf{x}, t) = \det(\mathbf{F}(\mathbf{x}, t)), \quad (4)$$

is the volume ratio⁴. In the presence of surface growth, distinction should be made between a point on the growth surface and the material point that happens to be at the same location at that instant. Let a point on the boundary of the body in the reference configuration be denoted by $\mathbf{x}_b(t)$, and its image in the physical configuration by $\mathbf{y}_b(t) = \hat{\mathbf{y}}(\mathbf{x}_b(t), t)$, the velocity of the boundary in the reference frame is then $\mathbf{V}^R = d\mathbf{x}_b/dt$, and the true velocity of the boundary in the physical space is $\mathbf{V} = d\mathbf{y}_b/dt$. By (3)¹ we can now write the velocity

⁴For simplicity, we will use the same notation, J , for both the volume ratio function expressed in terms of the reference frame coordinates, $J(\mathbf{x}, t)$, and the volume ratio function expressed in terms of the physical space coordinates, $J(\mathbf{y}, t)$.

of a solid unit that happens to be on the boundary ($\mathbf{x}_b(t)$) at the instant t as

$$\mathbf{v} = \mathbf{V} - \mathbf{F}\mathbf{V}^R. \quad (5)$$

Skalak et al. (1982, 1997) provide a careful discussion on the kinematics of surface growth. In particular, they refer to the velocity with which the material points move away from the surface of growth as the growth velocity

$$\mathbf{V}_G = \mathbf{v} - \mathbf{V} = -\mathbf{F}\mathbf{V}^R. \quad (6)$$

In the absence of growth, $\mathbf{V}_G = 0$ (or equivalently $\mathbf{V}^R = 0$), the boundary velocity and the material point velocity are equal. If a boundary is stationary in the physical space ($\mathbf{V} = 0$), the material velocity and the velocity of the boundary in the reference frame are related by $\mathbf{v} = -\mathbf{F}\mathbf{V}^R$.

In the general setting, the rate of addition of volume on the boundary of the body, per unit area, is thus

$$-\mathbf{V}_G \cdot \mathbf{n} \, dA_y = J\mathbf{V}^R \cdot \mathbf{n}^R \, dA_x, \quad (7)$$

where dA_y and dA_x denote the differential area elements in the physical and reference space, respectively, that are related by the deformation gradient through $\mathbf{n} \, dA_y = J\mathbf{F}^{-T}\mathbf{n}^R \, dA_x$, and with \mathbf{n} and \mathbf{n}^R denoting the corresponding outward pointing normal vectors. Hence, it is the normal component of the growth velocity that is associated with addition or removal of volume ($\mathbf{V}_G \cdot \mathbf{n} < 0$ corresponds to addition of volume) and from (7) it is apparent that addition or removal of volume in the reference configuration is directly related to the motion of the boundary ($\mathbf{V}^R \cdot \mathbf{n}^R > 0$ corresponds to addition of volume).

As pointed out by Skalak et al. (1982, 1997), the growth velocity \mathbf{V}_G need not be perpendicular to the growth surface, and various growth forms may arise due to different directions of \mathbf{V}_G . In this study, we restrict attention to the case of normal growth in the reference configuration where $\mathbf{V}^R = V^R \mathbf{n}^R$. This does not necessarily imply that in the physical space \mathbf{V}_G is normal to the boundary $\partial\mathcal{R}(t)$; the in-plane component of the boundary velocity in the reference frame is attributed to the velocity of material points due to shear deformations that can be either externally imposed or chemically induced.

3. Conservation laws and constitutive relations

The considered system is composed of two species, a solid matrix and a diffusing solvent. While on the boundaries of the body reactions of association or dissociation transform solvent units into solid units and vice versa, in any sub-region within the bulk either species must be separately conserved. Following the frameworks described in Fried and Gurtin (2004), Hong et al. (2008), Duda et al. (2010) and Chester and Anand (2010) we require that each species is separately incompressible, hence conservation of each species translates into conservation of volume.

Conservation of solvent. Let $\phi = \phi(\mathbf{y}, t)$ denote the solvent volume fraction in the physical configuration, and $\mathbf{j} = \mathbf{j}(\mathbf{y}, t)$ denote the true solvent flux (i.e. the volume of solvent

crossing a material unit area per unit time in the current configuration) the corresponding referential quantities $\phi^R = \phi^R(\mathbf{x}, t)$ and $\mathbf{j}^R = \mathbf{j}^R(\mathbf{x}, t)$ are related by the transformations

$$\phi^R = J\phi \quad \text{and} \quad \mathbf{j}^R = J\mathbf{F}^{-1}\mathbf{j}. \quad (8)$$

Then, within the body, conservation of solvent volume implies

$$\frac{\partial \phi}{\partial t} + \text{div}(\phi \mathbf{v} + \mathbf{j}) = 0, \quad (9)$$

in the current frame, or equivalently

$$\dot{\phi}^R + \text{Div}(\mathbf{j}^R) = 0, \quad (10)$$

in the reference frame.

Species balance. Since the solid units and the solvent units are separately incompressible, changes in the volume of a material region $\mathcal{D}(t)$ are solely due to the addition of solvent units. This can be written in integral form as

$$\frac{d}{dt} \int_{\mathcal{D}(t)} \phi dV_y = \int_{\partial \mathcal{D}(t)} \mathbf{v} \cdot \mathbf{n} dA_y, \quad (11)$$

and via usual integral transformations, can be rewritten in the local form as

$$\frac{\partial \phi}{\partial t} + \text{div}(\phi \mathbf{v}) = \text{div}(\mathbf{v}). \quad (12)$$

Combining the above relation with the requirement of conservation of solvent units in (9) we arrive at the compact form of the species balance requirement

$$\text{div}(\mathbf{v} + \mathbf{j}) = 0. \quad (13)$$

Additionally, transforming (12) into the reference space, yields

$$\dot{\phi}^R = \dot{J}, \quad (14)$$

and by integration we arrive at a relation between the referential solvent volume fraction and the swelling ratio in the form

$$\phi^R = J - 1, \quad (15)$$

where, by definition and without loss of generality, we have set $J \equiv 1$ for the dry state ($\phi^R = 0$). Combining (15) with the identity (8)¹ we obtain the species balance relation

$$J = \frac{1}{1 - \phi}, \quad (16)$$

which shows that the volume ratio of the solid matrix J serves as a measure of the swelling and we thus refer to it as the swelling ratio. Substituting (16) in (12), conservation of solvent

volume can be expressed in terms of J as

$$\frac{1}{J^2} \frac{\partial J}{\partial t} = \operatorname{div} \left(\frac{\mathbf{v}}{J} \right). \quad (17)$$

Finally, equations (9) and (13) are a sufficient and compact set of field equations to assure conservation of mass of both species in any subregion within the bulk of the body, with (16) relating between the volume ratio of the solid matrix and the solvent volume fraction. These equations must be complemented with considerations of mass conservation on the boundaries of the body.

Conservation of mass on the boundaries of the body. The association and dissociation reactions occurring on the boundaries of the body locally invalidate the requirement of species conservation. In other words, the flux of solvent flowing out⁵ of the body through a unit area on its boundary $\mathbf{j}^+ \cdot \mathbf{n} dA_y$ need not be equal to the flux of solvent flowing into the same unit area $\mathbf{j}^- \cdot \mathbf{n} dA_y$. Nonetheless, assuming that the chemical reaction is isochoric⁶, combined with the requirement that the species are separately incompressible, conservation of mass on the boundaries of the body translates to the requirement of volume conservation. Hence, returning to (13), in the presence of a singularity, conservation of volume across the surface reads

$$\llbracket (\mathbf{v} + \mathbf{j}) \cdot \mathbf{n} \rrbracket = 0, \quad (18)$$

where the square brackets denote the jump in the quantity across the boundary, such that $\llbracket () \rrbracket = ()^+ - ()^-$. Since there is no material on the outer side of the boundary, $\mathbf{v}^+ \equiv \mathbf{0}$ by definition. To write an equivalent form of the above relation in the reference frame, we first notice that it can be rewritten as

$$\llbracket \mathbf{j} \cdot \mathbf{n} \rrbracket = \llbracket (\mathbf{V} - \mathbf{v}) \cdot \mathbf{n} \rrbracket, \quad (19)$$

then, using (6), (7) and (8)², conservation of volume across the surface reads

$$\llbracket \mathbf{j}^R \cdot \mathbf{n}^R \rrbracket = (J - 1) \mathbf{V}^R \cdot \mathbf{n}^R. \quad (20)$$

Overall, the above equation (i.e. (19) or (20)) substitutes the requirements of species balance across the surface, by requiring that the local addition of solid volume is balanced by the local removal of solvent volume, to assure conservation of volume.

Mechanical equilibrium. Let $\mathbf{T} = \mathbf{T}(\mathbf{y}, t)$ and $\mathbf{S} = \mathbf{S}(\mathbf{x}, t)$ denote the Cauchy and Piola stress tensors respectively, mechanical equilibrium requires that

$$\operatorname{div} \mathbf{T} + \mathbf{b} = \mathbf{0}, \quad \mathbf{T} = \mathbf{T}^T, \quad (21)$$

$$\operatorname{Div} \mathbf{S} + \mathbf{b}^R = \mathbf{0}, \quad \mathbf{S} \mathbf{F}^T = \mathbf{F} \mathbf{S}^T, \quad (22)$$

⁵In the following, quantities on the outer and inner sides of the boundary surface are indicated by a superposed + and - sign, respectively.

⁶A non-isochoric reaction may be accounted for by introducing a local volume source.

where $\mathbf{b} = \mathbf{b}(\mathbf{y}, t)$ and $\mathbf{b}^R = \mathbf{b}^R(\mathbf{x}, t)$ denote the physical and referential body forces. Note that the Cauchy and Piola stress tensors are related by $\mathbf{S} = J\mathbf{T}\mathbf{F}^{-T}$ and the physical and referential body forces are related by $\mathbf{b}^R = J\mathbf{b}$.

Constitutive response. The energetic state of a material unit can be defined by the elastic deformation of the matrix (represented by the deformation gradient tensor \mathbf{F}) and the solvent concentration (represented by the solvent volume fraction ϕ^R). We thus represent the free energy per unit referential volume as

$$\psi = \psi(\mathbf{F}, \phi^R). \quad (23)$$

Then, using the Coleman-Noll methodology on the dissipation rate in a material subregion of the body, the constitutive relations can be derived. The Cauchy and Piola stresses read

$$\mathbf{T} = J^{-1} \frac{\partial \psi}{\partial \mathbf{F}} \mathbf{F}^T - p \mathbf{I}, \quad \mathbf{S} = \frac{\partial \psi}{\partial \mathbf{F}} - p J \mathbf{F}^{-T}, \quad (24)$$

respectively, and the chemical potential per unit reference volume is

$$\mu = \frac{\partial \psi}{\partial \phi^R} + p. \quad (25)$$

Here, since ϕ^R is associated with the concentration of solvent, the *hydrostatic pressure*⁷ p arises as a reaction to the constrain (4) and is constitutively indeterminate.

The dissipation in the bulk is solely due to diffusion of solvent, hence the dissipation rate argument leads to the inequality $\mathbf{j}^R \cdot \text{Grad } \mu \leq 0$. This inequality is satisfied by employing a kinetic law of the form

$$\mathbf{j}^R = -\mathbf{M}(\mathbf{F}, \phi^R) \text{Grad } \mu, \quad (26)$$

where the mobility tensor \mathbf{M} is positive semi-definite (i.e. $\mathbf{M}(\mathbf{F}, \phi^R) \mathbf{g} \cdot \mathbf{g} \geq 0$ for all vectors \mathbf{g}).

Notice that according to the above kinetic relation, finite values of flux require the chemical potential to be a continuous field. Specifically, this implies that on the boundaries of the body

$$[[\mu]] = 0, \quad (27)$$

thus relating the chemical potential in the surrounding solvent to that in the body, at the interface.

4. Driving force of growth

The constitutive equations in the previous section describe the large deformation mechanics of bodies composed of two species; a solid matrix and a diffusing solvent. To tie between the bulk response and the growth kinetics that are localized at boundaries of the body, we

⁷This pressure can alternatively be referred to as an *osmotic pressure*, since it does not necessarily vanish in absence of external loads and is a direct result of the species balance constrain that couples between the deformation of the solid matrix and the solvent intake.

return to the thermodynamic principles, and by considering the rate of dissipation associated with the growth reaction we seek to obtain the driving force that governs growth. Since this force is responsible for changes in the material configuration, it can also be thought of as a configurational force (Gurtin, 2008).

We begin by writing the dissipation rate in the physical space by integration over the entire region

$$\begin{aligned} \dot{D} = \int_{\partial\mathcal{R}(t)} \mathbf{T}\mathbf{n} \cdot \mathbf{V} dA_y + \int_{\mathcal{R}(t)} \mathbf{b} \cdot \mathbf{v} dV_y + \int_{\partial\mathcal{R}(t)} \mu \left[-\mathbf{j}^+ \cdot \mathbf{n} + (\mathbf{V} - \mathbf{v}) \cdot \mathbf{n} \right] dA_y \\ - \frac{d}{dt} \int_{\mathcal{R}(t)} \psi J dV_y, \end{aligned} \quad (28)$$

here the first two terms represent the power invested by the external loads acting on the boundary of the body⁸, and the body forces, respectively. The third term characterizes the rate of energy flux into the system per unit time due to solvent intake. The final term represents the rate of increase of the free energy of the system. Using the transformations (7) and (8)² the dissipation rate can be equivalently written in the reference frame, as

$$\begin{aligned} \dot{D} = \int_{\partial\mathcal{R}^R(t)} \mathbf{S}\mathbf{n}^R \cdot \mathbf{V} dA_x + \int_{\mathcal{R}^R(t)} \mathbf{b}^R \cdot \mathbf{v} dV_x + \int_{\partial\mathcal{R}^R(t)} \mu \left(-\mathbf{j}^{R+} \cdot \mathbf{n}^R + \mathbf{V}^R \cdot \mathbf{n}^R \right) dA_x \\ - \frac{d}{dt} \int_{\mathcal{R}^R(t)} \psi dV_x. \end{aligned} \quad (29)$$

Now we proceed to reorganize (29), to distinguish the dissipative mechanisms from the conservative terms. As a first step, we rewrite the first two terms in (29) by substituting relation (5), then by employing the divergence theorem and inserting the mechanical equilibrium relation (22) we arrive at the identity

$$\int_{\partial\mathcal{R}^R(t)} \mathbf{S}\mathbf{n}^R \cdot \mathbf{V} dA_x + \int_{\mathcal{R}^R(t)} \mathbf{b}^R \cdot \mathbf{v} dV_x = \int_{\partial\mathcal{R}^R(t)} \mathbf{S}\mathbf{n}^R \cdot \mathbf{F}\mathbf{V}^R dA_x + \int_{\mathcal{R}^R(t)} \mathbf{S} \cdot \dot{\mathbf{F}} dV_x. \quad (30)$$

Next, the third term in (29) can be rewritten with the aid of relation (20) to obtain

$$\int_{\partial\mathcal{R}^R(t)} \mu \left(-\mathbf{j}^{R+} \cdot \mathbf{n}^R + \mathbf{V}^R \cdot \mathbf{n}^R \right) dA_x = \int_{\partial\mathcal{R}^R(t)} \mu \left(-\mathbf{j}^{R-} \cdot \mathbf{n}^R + J\mathbf{V}^R \cdot \mathbf{n}^R \right) dA_x. \quad (31)$$

The first term in the above right-hand side integral can be further adapted by applying the divergence theorem and using relation (10) to write

$$\int_{\partial\mathcal{R}^R(t)} \mu \left(-\mathbf{j}^{R-} \cdot \mathbf{n}^R \right) dA_x = \int_{\mathcal{R}^R(t)} \left(-\mathbf{j}^{R-} \cdot \text{Grad } \mu + \mu \dot{\phi}^R \right) dV_x. \quad (32)$$

⁸Note that the velocity conjugate to the boundary traction is the boundary velocity \mathbf{V} and not the particle velocity \mathbf{v} .

There remains the final term that can be reexpressed using the transport theorem as

$$\frac{d}{dt} \int_{\mathcal{R}^R(t)} \psi dV_x = \int_{\mathcal{R}^R(t)} \dot{\psi} dV_x - \int_{\partial\mathcal{R}^R(t)} \Delta\psi \mathbf{V}^R \cdot \mathbf{n}^R dA_x, \quad (33)$$

where

$$\Delta\psi = \psi^+ - \psi^-, \quad (34)$$

represents the jump in potential energy density across the moving boundary. This difference will be referred to as the latent energy of growth. It arises due to the mechanism of local energy transduction associated with the phase transformation (from solvent phase into the solid phase or vice versa).

Recalling that the free energy density $\psi = \psi(\mathbf{F}, \phi^R)$ is taken to be a function of the deformation gradient tensor \mathbf{F} and the referential volume fraction ϕ^R , we can write

$$\dot{\psi} = \frac{\partial\psi}{\partial\mathbf{F}} \cdot \dot{\mathbf{F}} + \frac{\partial\psi}{\partial\phi^R} \dot{\phi}^R = \mathbf{S} \cdot \dot{\mathbf{F}} + \mu \dot{\phi}^R. \quad (35)$$

Now, by substituting relations (30)-(33) and (35) in (29) and reorganizing, the dissipation rate reads

$$\dot{D} = \int_{\partial\mathcal{R}^R(t)} (\mathbf{F}^T \mathbf{S} + \Delta\psi \mathbf{I} + \mu J \mathbf{I}) \mathbf{n}^R \cdot \mathbf{V}^R dA_x - \int_{\mathcal{R}^R(t)} \mathbf{j}^R \cdot \text{Grad } \mu dV_x. \quad (36)$$

Here the two integrals characterize the two different mechanisms of energy dissipation: the surface integral is associated with dissipation on the boundary and the volume integral with dissipation in the bulk due to the diffusion of solvent through the solid matrix.

The constitutive relation in (26) assures us that the dissipation rate associated with diffusion is non-negative, hence the remaining inequality that must be satisfied to guarantee a non-negative dissipation rate, is

$$\int_{\partial\mathcal{R}^R(t)} (\mathbf{F}^T \mathbf{S} + \Delta\psi \mathbf{I} + \mu J \mathbf{I}) \mathbf{n}^R \cdot \mathbf{V}^R dA_x \geq 0. \quad (37)$$

As explained in Section 2, in the present study we restrict attention to the case of normal growth in the reference configuration such that, $\mathbf{V}^R = V^R \mathbf{n}^R$. Recall that this restriction does not necessarily imply normal growth in the physical configuration, but excludes growth induced shear deformations at the surface. Hence, the dissipation inequality (37) can be rewritten as

$$\int_{\partial\mathcal{R}^R(t)} (\mathbf{S} \mathbf{n}^R \cdot \mathbf{F} \mathbf{n}^R + \Delta\psi + \mu J) V^R dA_x \geq 0. \quad (38)$$

Finally, from the above relation we identify the thermodynamic conjugate to the growth rate ($V^R = \mathbf{V}^R \cdot \mathbf{n}^R$) which is the *driving force of growth* that acts along the growth direction (per unit reference area)

$$f = \mathbf{S} \mathbf{n}^R \cdot \mathbf{F} \mathbf{n}^R + \Delta\psi + \mu J. \quad (39)$$

The dissipation inequality (38) thus reduces to the requirement

$$fV^R \geq 0 \quad \text{on} \quad \partial\mathcal{R}^R(t). \quad (40)$$

Recalling that the boundary velocity in the reference frame is such that $V^R > 0$ for association, and $V^R < 0$ for dissociation, we thus infer from inequality (40) that the driving force is positive $f > 0$ for association, and negative $f < 0$ for dissociation.

Examining the driving force relation (39) we identify three terms. The first term is associated with mechanical forces acting on the boundary. The second term is the latent energy of the growth reaction and the third term is the influx of chemical energy. These three effects act together to define the kinetics of surface growth. Note that a similar result for the driving force was obtained by Tomassetti et al. (2016). Therein, the coupling between growth and diffusion was accounted for through an external field and not coupled to the mechanical response, hence the difference in the driving force terms.

Kinetic law of growth. In light of inequality in (40) a specific form of the kinetic law that governs growth can be chosen as

$$V^R = \mathcal{G}(f), \quad (41)$$

where the growth function $\mathcal{G}(f)$ obeys the inequality $f\mathcal{G}(f) \geq 0$ for all values of f .

5. Summary of formulation and specific constitutive equations

In the previous sections we have developed a complete formulation of the mechanics of a body composed of two species (i.e. solid and solvent) that can grow by combination of two mechanisms (i.e. swelling and surface growth). In the physical space, the body is described in spatial coordinates \mathbf{y} , and its boundaries \mathbf{y}_b have velocity \mathbf{V} . Equivalently, in the reference frame, the body can be described using coordinates \mathbf{x} and \mathbf{x}_b and the boundary velocity \mathbf{V}^R . Fields \mathbf{v} , \mathbf{F} and J are key to relate between the two configurations and to thus define the state of the body. Mass conservation in the physical space is governed by the continuity equation (9), the incompressibility argument (13) and the species balance (16), to link the fields \mathbf{v} and J to the solvent volume fraction ϕ and the solvent flux \mathbf{j} . Or equivalently, in the reference space, equations (10) and (15) relate J to ϕ^R and \mathbf{j}^R . Mechanical equilibrium is accounted for in the current configuration through (21), and in the reference configuration through (22). The stress tensors \mathbf{T} , \mathbf{S} and chemical potential μ obey the constitutive relations (24) and (25), respectively and depend on a specific form of the free energy $\psi(\mathbf{F}, \phi^R)$. The diffusion law (26) relates the referential flux \mathbf{j}^R to the gradient of chemical potential through a mobility tensor $\mathbf{M}(\mathbf{F}, \phi^R)$ and the physical flux \mathbf{j} can be derived through the equivalence relation (8)².

On the boundaries of the body, we shall account for the volume conservation across the surface (18), the continuity of chemical potential (27), and the applied loads or physical constraints. The density of material growing on a given growth surface is a property of this surface (it can be influenced by surface roughness and chemical binding properties). This surface density predetermines the tangential deformation of the solid matrix on the association surface and provides an additional boundary condition. Finally, the kinetic law of growth $\mathcal{G}(f)$ must be defined to determine the growth kinetics and is related to the driving force (39) and the growth velocity (41).

In summary, for a given material characterized by a constitutive response defined by ψ and \mathbf{M} , the kinetic relation \mathcal{G} is the only additional constitutive relation needed to specialize the growth kinetics to a specific problem. Before we proceed to apply our model to a boundary-value problem we thus choose a specific set of constitutive relations. We consider a setting in which the grown material is a polymer gel that is composed of a polymer network and an impregnating solvent that contains monomers. Polymer gels that can grow and swell are of particular interest due to their ubiquity in natural systems, additionally they have been shown to associate and dissociate on their boundaries in artificial settings (Noireaux et al., 2000; Bauër et al., 2017) thus providing a model system for the investigation of chemo-mechanically coupled growth.

Constitutive response in the bulk. To account for both finite stretching of the polymer network and for species migration, we employ a constitutive framework for the bulk response based on the models suggested by Hong et al. (2008), Chester and Anand (2010), and Duda et al. (2010) with some minor modifications in their representation.

We construct the Helmholtz free energy following the Flory and Rehner (1943) approach by accounting separately for the contribution of each species to write

$$\psi(\mathbf{F}, \phi^R) = \psi_e(\mathbf{F}) + \psi_s(\phi^R), \quad (42)$$

where $\psi_e(\mathbf{F})$ represents the free energy of the solid matrix due to elastic deformation, and $\psi_s(\phi^R)$ represents the free energy of the solvent and depends on the fraction of solvent within a volume unit given by J . The former is taken as (Treloar, 1975)

$$\psi_e(\mathbf{F}) = \frac{G}{2} [|\mathbf{F}|^2 - 3 - 2 \ln(\det \mathbf{F})], \quad G = NkT, \quad (43)$$

where G is the elastic shear modulus, N represents the number of solid chains per unit volume of the body, k is the Boltzmann's constant, and T is the temperature.

Assuming that the unmixed solvent in the surrounding region is in chemical equilibrium, it has a constant chemical potential μ_0 and due to incompressibility, the free energy of a unit volume of unmixed solvent is $\psi_0 = \mu_0$. Once the solvent penetrates into the solid matrix it changes its free energy (per unit volume) by both change in relative volume and by mixing. The free energy of mixing is assumed to have the form proposed by Flory (1942) and thus the total free energy associated with the impregnating solvent is

$$\psi_s(\phi^R) = \phi^R \left\{ \psi_0 + \frac{kT}{\nu} \left[\ln \left(1 - \frac{1}{1 + \phi^R} \right) + \frac{\chi}{1 + \phi^R} \right] \right\}, \quad (44)$$

where χ represents the Flory-Huggins interaction parameter and ν the volume of a solvent unit. Substituting the expression of the Helmholtz free energy (42) (with (43) and (44)) in (24) and (25), and using the relation (15), we can now write the Cauchy and Piola stress tensors as

$$\mathbf{T} = \frac{G}{J} \left[\mathbf{F}\mathbf{F}^T - \left(1 + J \frac{p}{G} \right) \mathbf{I} \right], \quad \mathbf{S} = G \left[\mathbf{F} - \left(1 + J \frac{p}{G} \right) \mathbf{F}^{-T} \right], \quad (45)$$

respectively, and the chemical potential as

$$\mu = \mu_0 + \frac{kT}{\nu} \left[\ln \left(1 - \frac{1}{J} \right) + \frac{1}{J} + \frac{\chi}{J^2} \right] + p. \quad (46)$$

The solvent diffusion within the solid matrix is assumed to follow the classical model (Feynman et al., 1963) that has the form

$$\mathbf{j} = -\frac{D\nu}{kT} \phi \text{ grad } \mu, \quad (47)$$

where D is the diffusion coefficient. The diffusion is hence proportional to the gradient of chemical potential and to the solvent volume fraction. The referential and spatial gradients are related by $\text{Grad } \mu = \mathbf{F}^T \text{ grad } \mu$. Thus the referential description of the kinetic law above corresponds to a mobility tensor, defined in (26), of the form

$$\mathbf{M}(\mathbf{F}, \phi^R) = \frac{D\nu}{kT} \phi^R \mathbf{B}^{-1} \quad \text{where} \quad \mathbf{B} = \mathbf{F}^T \mathbf{F}. \quad (48)$$

Note that \mathbf{M} is symmetric and positive definite provided that $D > 0$.

A full description of the material response in the bulk is thus defined by a set of material parameters $(\nu, N, \chi, \psi_0, D)$. In solving a specific growth problem in the next section we will use common values of the model parameters found in the literature: $\nu = 10^{-28} \text{m}^3$, $N = 10^{24} \text{m}^{-3}$, $\chi = 0.2$ and $\psi_0 = -4 \times 10^5 \text{Jm}^{-3}$, and assuming room temperature we have $kT = 4 \times 10^{-21} \text{J}$. Investigation of the constitutive sensitivity of our results will center on model parameters that are associated with growth kinetics, and will thus include the influence of diffusion rates that are dictated by the diffusion coefficient D .

Constitutive relations on the boundary. The latent energy of growth is defined as the jump of potential energy across the boundary (34). On the inner side of the boundary (within the body), the free energy is defined by equation (42). Considering an impermeable growth surface, association on this boundary is promoted by a chemical binding potential that locally alters the potential energy, such that $\psi^+ = \psi_a$, and represents the energetic gain due to association. Therefore, the latent energy of association reads

$$\Delta\psi = \psi_a - \psi. \quad (49)$$

At the dissociation surface material on the inner side of the boundary (within the body) has free energy $\psi^- = \psi$ and a volume ratio of J ; the same volume of material on the outer side of the boundary (in the solvent region) has a free energy of $\psi^+ = J\psi_0$. The latent energy at the dissociation surface is thus

$$\Delta\psi = J\psi_0 - \psi. \quad (50)$$

Notice that in this case, we assume that the dissociation happens naturally and is not prompted by a local energy.

The remaining constitutive relation that needs to be defined is the kinetic law of growth (41), or in other words, the growth function $\mathcal{G}(f)$. Although the present study is concerned with modeling surface growth phenomena from a macroscopic point of view by applying

tools of continuum mechanics, the surface growth reaction occurs locally and is driven by a *Brownian Ratchet* mechanism of polymerization/depolymerization; a process governed by random walks and thermal fluctuations (Mogilner and Oster, 1996, 2003a,b; Theriot, 2000). Nonetheless, by observing biological growth, it is apparent that the stochastic nature of these processes at the microscopic level does not transcend into the macroscopic response. Here we apply the relation for the driving force (39) to tie between the locally occurring chemo-mechanical process, and the deterministic response at the macroscopic level.

We consider a simplified framework in which chemical reactions take place only at the free ends of the polymer network that are exposed at the boundaries of the body. The intrinsic polarity of the solid matrix is such that the reaction rates are different at either end (Theriot, 2000). When considering polymerization, the rate of association is typically referred to as r_{on} while the rate of dissociation as r_{off} . The absolute rate of growth is thus regularly written in the form $r = r_{\text{on}} - r_{\text{off}}$. Hence, for association we have $r > 0$ while for dissociation $r < 0$. We can relate these reaction rates with the energy barrier that must be overcome to induce them, which is the work invested by the driving force in binding/unbinding a single unit, i.e. νf . Therefore, we can describe the thermally activated process by applying a growth function of an Arrhenius form

$$\mathcal{G}(f) = \frac{b}{2} \left(e^{\frac{\nu f}{kT}} - e^{-\frac{\nu f}{kT}} \right) = b \sinh \left(\frac{\nu f}{kT} \right), \quad (51)$$

that obeys the thermodynamic inequality (40) for a reaction constant $b > 0$, which according to (41), scales with the growth rate. Here, each exponential corresponds to a different reaction. The first exponential represents r_{on} and the second exponential represents r_{off} . In the limit of small departures from thermodynamic equilibrium, (51) reduces to the linear form

$$\mathcal{G}(f) = b \left(\frac{\nu f}{kT} \right). \quad (52)$$

In the present study we choose the kinetic law of growth to be identical for both the association and dissociation surfaces and introduce the polarity through the latent energy of growth (49) and (50). This formulation allows the growth surfaces to smoothly transition from association to dissociation and vice versa if it becomes energetically favorable.

6. A boundary-value problem: Growth on a flat surface

The theoretical framework presented in the previous sections can be applied to study coupled growth processes occurring in an arbitrary geometry. In this section, we demonstrate its application for the specific problem of growth on a flat substrate. It will be shown that this simple growth setting generates nontrivial insights into the kinetics of surface growth with coupled diffusion. Moreover, it provides a good approximation for growth of thin layers on surfaces of arbitrary geometry.

As for the derivation of the general model, in solution of the specific boundary value problem we make use of both the physical and referential spaces. The physical space is described by the set of axis (y_1, y_2, y_3) where the y_1 -axis is perpendicular to the rigid substrate.

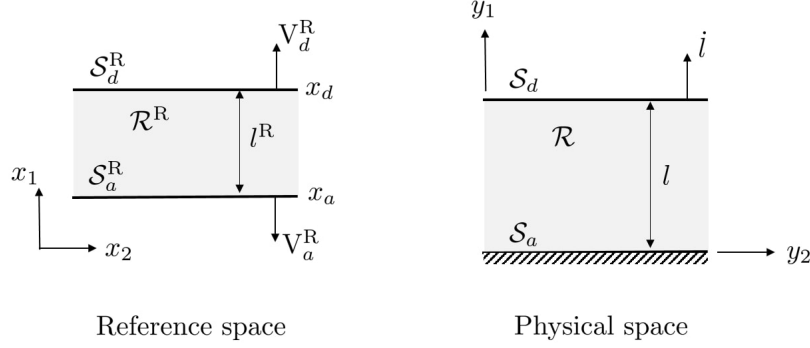


Figure 2: Continuum representation of a body grown on an infinite flat surface in the reference space and in the physical space.

At a given time t , the body manifold occupies the region

$$0 \leq y_1 \leq l(t), \quad -\infty < y_2, y_3 < +\infty, \quad (53)$$

where $l(t)$ is the thickness of the body (Fig. 2). Association occurs on the substrate $y_1 = 0$ and dissociation occurs on the free surface $y_1 = l(t)$.

The reference space is described by the set of axis (x_1, x_2, x_3) where the x_1 -axis is perpendicular to the association surface. At a given time t , the material manifold occupies the region

$$x_a(t) \leq x_1 \leq x_d(t), \quad -\infty < x_2, x_3 < +\infty, \quad (54)$$

where $x_1 = x_a(t)$ and $x_1 = x_d(t)$ represent the association and dissociation surfaces respectively.

We consider a situation in which growth is promoted on the substrate by a homogeneous density of binding sites that imposes a constant equibiaxial in-plane stretch λ_0 of the grown material. The mapping from the reference to the current configuration (2) thus reduces to the form

$$y_1 = \hat{y}_1(x_1, t), \quad y_2 = \lambda_0 x_2, \quad y_3 = \lambda_0 x_3, \quad (55)$$

and the swelling ratio can be expressed as

$$J = \lambda \lambda_0^2, \quad (56)$$

where λ denotes the out-of plane stretch

$$\lambda(x_1, t) = \frac{\partial \hat{y}_1}{\partial x_1}. \quad (57)$$

For future use we denote the swelling ratios at the association and dissociation boundaries by $J_a = J(y_1 = 0, t)$ and $J_d = J(y_1 = l, t)$, respectively.

Since all of the motion occurs along the growth direction, the material velocity and flux can be written as $\mathbf{v} = v(x_1, t)\mathbf{e}_{y_1}$ and $\mathbf{j} = j(x_1, t)\mathbf{e}_{y_1}$ where

$$v(x_1, t) = \frac{\partial \hat{y}_1}{\partial t}. \quad (58)$$

In this setting, the velocity of the association and dissociation surfaces in the current configuration are

$$\mathbf{V} = \mathbf{0} \quad \text{and} \quad \mathbf{V} = \dot{l} \mathbf{e}_{y_1}, \quad (59)$$

respectively. Similarly in the reference configuration the boundary velocities are

$$\mathbf{V}^R = -V_a^R \mathbf{e}_{x_1} \quad \text{and} \quad \mathbf{V}^R = V_d^R \mathbf{e}_{x_1}, \quad (60)$$

where V_a^R and V_d^R denote the referential association and dissociation velocities respectively.

Now, let $l^R(t)$ denote the thickness of the growing layer in the reference frame, that we will refer to as the *dry thickness*, its time derivative can be expressed in terms of association and dissociation rates as

$$\dot{l}^R = V_a^R + V_d^R. \quad (61)$$

Turning to considerations of mass conservation, we combine conservation equation (13) with the jump condition (18) on the impermeable association surface, to relate the material velocity and the solvent flux by

$$v + j = 0, \quad (62)$$

and equation (17) specialized to this uniaxial problem yields

$$\frac{\partial J}{\partial t} = J^2 \frac{\partial}{\partial y_1} \left(\frac{v}{J} \right). \quad (63)$$

Employing the constitutive relation (45) we can obtain the principal Cauchy stress components

$$T_{11} = NkT \left(\frac{J}{\lambda_0^4} - \frac{1}{J} \right) - p, \quad T_{22} = NkT \left(\frac{\lambda_0^2}{J} - \frac{1}{J} \right) - p. \quad (64)$$

In the absence of body forces, mechanical equilibrium (21) implies that the out-of-plane stress vanishes through the thickness of the body ($T_{11} = 0$), hence the hydrostatic pressure as a function of the swelling ratio is

$$p(J) = NkT \left(\frac{J}{\lambda_0^4} - \frac{1}{J} \right). \quad (65)$$

The in-plane stress component (64)² is non-zero and can now be written as

$$T_{22} = NkT \left(\frac{\lambda_0^2}{J} - \frac{J}{\lambda_0^4} \right), \quad (66)$$

and similarly the chemical potential (46) reads

$$\mu(J) = \mu_0 + \frac{kT}{\nu} \left[\ln \left(1 - \frac{1}{J} \right) + \frac{1}{J} + \frac{\chi}{J^2} \right] + NkT \left(\frac{J}{\lambda_0^4} - \frac{1}{J} \right). \quad (67)$$

Using to (15) to relate ϕ^R to J , and (55) and (56) to relate the components of \mathbf{F} to J , the free energy given in (42), (43) and (44) can also be expressed as a function of J as follow

$$\psi(J) = \frac{NkT}{2} \left(\frac{J^2}{\lambda_0^4} + 2\lambda_0^2 - 3 - 2 \ln J \right) + (J-1) \left\{ \psi_0 + \frac{kT}{\nu} \left[\ln \left(1 - \frac{1}{J} \right) + \frac{\chi}{J} \right] \right\}. \quad (68)$$

As a result, the driving force at the boundary (39) can be written as a function of J in the form

$$f(J) = \Delta\psi(J) + \mu(J)J. \quad (69)$$

Corresponding relations for the driving force at the association and dissociation boundaries $f(J_a)$ and $f(J_d)$, respectively, are found in (B2) and (B3) of Appendix B. Consequently, by the kinetic law (51), the association and dissociation rates are also functions of J , namely $V_a^R = V_a^R(J_a)$ and $V_d^R = V_d^R(J_d)$.

Now, using the diffusion law (47) and relation (62), we can express the ratio v/J as

$$\frac{v}{J} = \Lambda(J) \frac{\partial J}{\partial y_1} \quad \text{where} \quad \Lambda(J) = \frac{D\nu}{kT} \left(\frac{J-1}{J^2} \right) \frac{d\mu}{dJ}. \quad (70)$$

By substituting the specific expression of the chemical potential (67) we can write

$$\Lambda(J) = D \left[\frac{N\nu}{\lambda_0^4} \frac{1}{J} - \frac{N\nu}{\lambda_0^4} \frac{1}{J^2} + N\nu \frac{1}{J^3} + (1 - N\nu - 2\chi) \frac{1}{J^4} + 2\chi \frac{1}{J^5} \right]. \quad (71)$$

The combination of the two equations (63) and (70) results in a single partial differential equation for the field variable $J(y_1, t)$, which is sufficient to determine the response in the bulk. To complete the representation of the boundary value problem, it remains to determine the values of J on the association and dissociation surfaces. The coupling between surface growth and swelling is generated by the dependence of the association and dissociation reactions on the local values of the field J . To formulate this dependence, let us first examine the dissociation boundary. The continuity of chemical potential (67) at $y_1 = l(t)$ implies

$$\mu(J_d) = \mu_0, \quad (72)$$

thus resulting in an implicit relation for J_d (provided in full form (B1) in Appendix B). Holding the reference chemical potential of the surrounding solvent μ_0 constant, J_d is also constant in time, and is dictated by material parameters (χ , N , ν), and the in-plane bi-axial stretch λ_0 .

By the kinematic relation (5), the particle velocity at the dissociation boundary is

$$v_d = \dot{l} - \frac{J_d}{\lambda_0^2} V_d^R(J_d), \quad (73)$$

notice that the dissociation rate $V_d^R = V_d^R(J_d)$ is constant in time.

Now let us examine the association boundary. The material velocity v_a at the interface

can be written with the aid of the kinematic relation (5) as a function of J_a

$$v_a = \frac{J_a}{\lambda_0^2} V_a^R(J_a). \quad (74)$$

The combination of (70) and (74) implies a boundary condition on the association surface that couples the kinetics of association to the swelling ratio by

$$\Lambda(J) \frac{\partial J}{\partial y_1} - \frac{V_a^R(J_a)}{\lambda_0^2} = 0 \quad \text{at} \quad y_1 = 0. \quad (75)$$

Finally, the governing equations can be summarized in the physical space by the boundary value problem

$$\begin{cases} \frac{\partial J}{\partial t} = J^2 \frac{\partial}{\partial y_1} \left(\Lambda(J) \frac{\partial J}{\partial y_1} \right), & 0 \leq y_1 \leq l(t) \\ \llbracket \mu(J) \rrbracket = 0, & y_1 = l(t) \\ \Lambda(J) \frac{\partial J}{\partial y_1} - \frac{V_a^R(J)}{\lambda_0^2} = 0, & y_1 = 0 \end{cases} \quad (76)$$

where $l(t)$ is given by (73). Alternatively, we can write the problem in the reference space with the following equations

$$\begin{cases} \dot{J} = \frac{\partial}{\partial x_1} \left(\lambda_0^4 \Lambda(J) \frac{\partial J}{\partial x_1} \right), & x_a(t) \leq x_1 \leq x_d(t) \\ \llbracket \mu(J) \rrbracket = 0, & x_1 = x_d(t) \\ \lambda_0^4 \Lambda(J) \frac{\partial J}{\partial x_1} - J V_a^R(J) = 0, & x_1 = x_a(t) \end{cases} \quad (77)$$

where J refers to the swelling ratio expressed either in the reference space coordinates or the physical space coordinates indifferently. Hence, we have reduced the problem to be fully defined by a single field variable, the swelling ratio, and the time dependent thickness of the layer, which can be written in the current or reference configurations, as $(l(t), J(y_1, t))$ or $(l^R(t), J(x_1, t))$, respectively. Once the field J is known, all other fields (deformation, stresses, chemical potential) can be identified.

While both of the representations are equivalent, a specific advantage of the reference frame is in allowing us to separate the two species, since the dry thickness $l^R(t)$ indicates the amount of solid solely. Nonetheless, in the following sections, we will alternate between both configurations.

Although the considered growth process is highly nonlinear, to obtain a better understanding of the time and length scales associated with growth we observe that from the differential equation of (77) with (71), the diffusion rate in gels with finite swelling scales with $(DN\nu)/L$, where L is the characteristic dry length of the system. On the other hand, according to (51) the growth rate scales with b . However, from the second boundary condition in (77) along with the identity (16), it is evident that these rates are not independent and the ratio between them is ultimately dictated by the local swelling gradients that are generated by the growth reaction

$$\frac{\partial \phi^R}{\partial \xi_1} \propto \frac{bL}{DN\nu} = \frac{L}{l_c}, \quad (78)$$

where $\xi_1 = x_1/L$ and the critical length scale is defined as $l_c = DN\nu/b$. In other words, if the layer thickness is much smaller than the critical length ($L \ll l_c$), the swelling gradients are small thus suppressing diffusion, and if the layer thickness is much larger than the critical length ($L \gg l_c$), swelling gradients at the association boundary accelerate the diffusion to sustain the growth. Hence, the rate coefficients (i.e. D and b) dictate the critical length scale, and determine the local gradients of swelling needed to sustain the growth. However, since the material is growing, the characteristic length scale of the system can significantly change throughout the process and the time scales vary accordingly.

Treadmilling response. If addition and removal of mass are balanced, the system will arrive at a treadmilling regime, a steady state in which the layer thickness is constant although association and dissociation are continuously occurring. Once the system has arrived at this the treadmilling state, all time derivatives in the current configuration vanish. Therefore, the boundary value problem (76) can be solved analytically to determine the steady thickness \tilde{l} and the steady swelling ratio field $\tilde{J}(y_1)$, where the superscript $(\tilde{})$ denotes treadmilling values.

According to (61), once addition and removal of solid mass are balanced, we can write

$$V_a^R(\tilde{J}_a) = -V_d^R(\tilde{J}_d), \quad (79)$$

where $\tilde{J}_a = \tilde{J}(y_1 = 0)$ denotes the steady swelling ratio at the association boundary. Since V_d^R is constant, \tilde{J}_a can be determined from (79) with V_a^R and V_d^R related to the driving force (69) by the kinetic relation (51).

Combining (79) with (76), in absence of time dependence, a differential equation for the steady field \tilde{J} can be obtained

$$\Lambda(\tilde{J}) \frac{d\tilde{J}}{dy_1} = \frac{V_a^R(\tilde{J}_a)}{\lambda_0^2}, \quad (80)$$

which by integration yields an implicit relation between the swelling ratio \tilde{J} and the spatial coordinate y_1

$$y_1(\tilde{J}) = \frac{\lambda_0^2}{V_a^R(\tilde{J}_a)} \int_{\tilde{J}_a}^{\tilde{J}} \Lambda(J) dJ. \quad (81)$$

The stationary thickness in the physical space can thus be derived as

$$\tilde{l} = y_1(J_d). \quad (82)$$

Although in the reference frame the boundaries of the body at treadmilling move at a constant velocity given by (79), the distance between any two spatial points mapped back into the reference frame remains constant, due to self-similarity. Therefore, employing the inverse transformation $x_1 = \hat{x}_1(y_1, t)$, we define the distance from the association surface in the reference frame as $\Delta x_1 = \hat{x}_1(y_1, t) - \hat{x}_1(0, t)$ which by integration of the transformation (57) reads

$$\Delta x_1 = \int_0^{y_1} \frac{\lambda_0^2}{\tilde{J}(y_1)} dy_1. \quad (83)$$

Now we substitute equation (80) to obtain an implicit relation between the steady field \tilde{J}

and the distance Δx_1

$$\Delta x_1(\tilde{J}) = \frac{\lambda_0^4}{V_a^R(\tilde{J}_a)} \int_{\tilde{J}_a}^{\tilde{J}} \frac{\Lambda(J)}{J} dJ. \quad (84)$$

The dry thickness \tilde{l}^R is then given by

$$\tilde{l}^R = \Delta x_1(J_d). \quad (85)$$

Analytical relations for $y_1(\tilde{J})$ and $\Delta x_1(\tilde{J})$ are given in relations (B4) and (B5) of Appendix B.

Integration results and parameter sensitivity. Given the above formulation, the steady state, if reached, is unique and characterized by $(\tilde{l}, \tilde{J}(y_1))$ in the physical frame, or alternatively by $(\tilde{l}^R, \tilde{J}(\Delta x_1))$ in the reference frame. To study the effect of model parameters that are associated with the growth kinetics on the treadmilling response, we hold the material parameters defined in the previous section (ν , N , χ , ψ_0) constant, and examine the variation of $(\tilde{l}^R, \tilde{J}(\Delta x_1))$ with the kinetic parameters, namely the diffusion coefficient - D , the reaction constant - b and the potential energy gain at the association surface - ψ_a .

First, from equations (84) and (85), along with the kinetic law (51), it is observed that V_d^R is proportional to b while $\Lambda(J)$ is proportional to $DN\nu$ (by its definition in equation (71)), hence the lengths Δx_1 and \tilde{l}^R scale with the critical length l_c defined in (78). On the other hand, the swelling ratio \tilde{J}_a is not affected by the rate coefficients (D and b), as observed from equation (79), nor is the distribution of the treadmilling swelling ratio \tilde{J} . In the following sections we take $DN\nu = 10^{-8}\text{m}^2\text{s}^{-1}$ and $b = 10^{-7}\text{ms}^{-1}$; the critical length is thus $l_c = 10^{-1}\text{m}$.

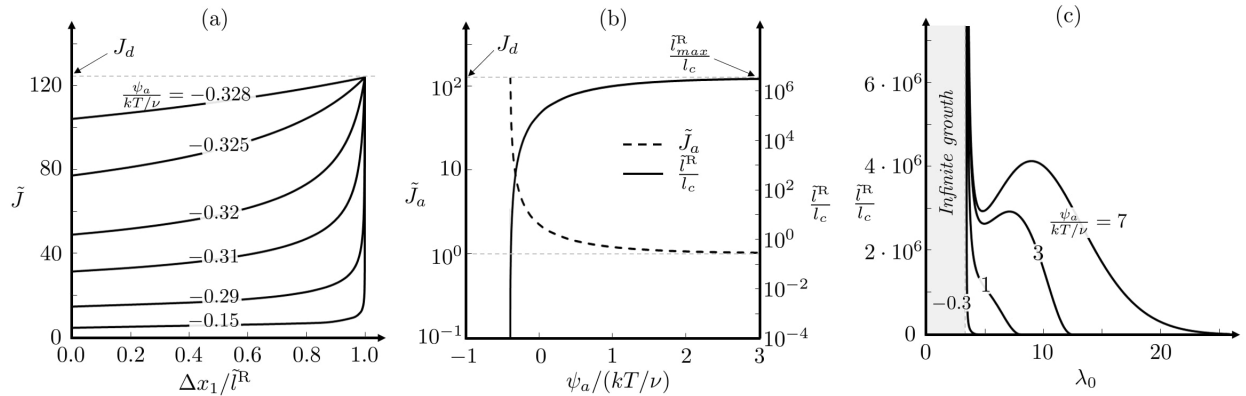


Figure 3: Sensitivity of treadmilling response to growth parameters: (a) Distribution of swelling through the layer ($\Delta x_1/\tilde{l}^R$) for various values of the potential energy gain at the association surface ψ_a with $\lambda_0 = 4.96$. (b) Swelling ratio at the association surface \tilde{J}_a and the dimensionless thickness \tilde{l}^R/l_c as a function of the dimensionless potential energy gain $\psi_a/(kT/\nu)$, with $\lambda_0 = 4.96$. Logarithmic scales are used to present the swelling ratio and the dimensionless thickness (c) Dry thickness as a function of the in-plane stretch at the association boundary λ_0 for various values of ψ_a .

The potential energy gain at the association boundary ψ_a has a more complex effect on the treadmilling response. In Fig. 3(a) we show curves for the treadmilling swelling

ratio as a function of the normalized distance from the association surface in the reference frame $\Delta x_1/\tilde{l}^R$, for various values of $\psi_a/(kT/\nu)$. It is observed that as ψ_a increases the swelling ratio at the association boundary decreases and swelling gradients localize near the dissociation boundary. From the limited range of ψ_a values in Fig. 3(a), it is apparent that the energy ψ_a has to fall within a certain range for growth to be both physically possible and energetically favorable. First the steady dry thickness needs to have a positive value $\tilde{l}^R \geq 0$, which, by combination of (84) and (85), requires J to be an increasing function thus leading to the inequality $\tilde{J}_a \leq J_d$, that defines a lower bound limit such that $\psi_a \geq -0.329(kT/\nu)$, as derived from equation (79). Although there is no physical upper bound limit on the value of ψ_a , it is found that as ψ_a increases beyond the range presented in Fig. 3(a) changes become insignificant while the swelling ratio at the association boundary tends to the incompressibility limit $\tilde{J}_a \rightarrow 1$. Hence, beyond a certain limit the treadmill response becomes insensitive to ψ_a . This point is further explained by the curves presented in Fig. 3(b), where we show the dependence of the association swelling ratio \tilde{J}_a and the dimensionless treadmill length \tilde{l}^R/l_c on $\psi_a/(kT/\nu)$. First we notice that when ψ_a approaches its lower bound, the thickness of the layer vanishes such that $\tilde{l}^R \rightarrow 0$ and $\tilde{J}_a \rightarrow J_d$. On the other hand, as ψ_a increases, $\tilde{J}_a \rightarrow 1$, and the thickness of the layer approaches an asymptotic limit $\tilde{l}^R \rightarrow \tilde{l}_{max}^R$ (which can be determined analytically via (84) and (85) with $\tilde{J}_a = 1$). Physically, a higher association energy enhances the association reaction by kinetic law (51), thus leading to a larger steady dry thickness, however this becomes inefficient as the solid matrix becomes more dense thus resisting the flux of solvent that is needed to generate growth. At the limit ($\psi_a \rightarrow \infty$) solvent cannot reach the association surface thus choking the growth.

Next we explore the sensitivity of \tilde{l}^R to the in-plane stretch λ_0 that is dictated by the properties of the growth surface. It is worth emphasizing that for a given set of material parameters, λ_0 is the only tuneable parameter that can be adjusted to determine the growth. In natural systems, λ_0 is controlled by the distribution of binding sites on the growth surface (recall that $1/\lambda_0$ is the fraction of solid volume generated on the growth surface). From Fig. 3(c) it is immediately noticed that λ_0 has a nonintuitive effect on the growth. If the growth reaction is sparse and $\lambda_0 \gg 10$ then dissociation becomes energetically favorable and the thickness of the layer vanishes. At the other end, if the growth reaction is dense ($\lambda_0 < 3.5$), this leads to smaller values of J_d , which by (69) result in a change of sign of the driving force so that it becomes energetically favorable to associate at the free boundary. Hence, association occurs on both boundaries and the layer will continue to grow indefinitely. In the intermediate zone ($\lambda_0 > 3.5$) the rate of dissociation increases monotonically with increasing λ_0 , thus contributing to the reduction in maximum thickness, however we observe a non-monotonic dependence on λ_0 as ψ_a increases: first a local minimum appears then a local maximum is observed. This behaviour is due to the competition between two effects: increasing values of ψ_a favor growth, while increasing values of λ_0 hinder it. To further understand this complex response it is essential to consider the evolution of the growth before it has arrived at the treadmill state.

Numerical results and the emergence of a universal path. Although it has been established in the previous section that, under certain conditions, a treadmill response can exist, it has yet to be determined whether and how the boundary value problem, defined by (76) and (77), evolves towards this treadmill state. Is this evolution sensitive to initial

conditions? And more importantly, how does a layer evolve from an initial state with no solid at all? In other terms, can this model capture the entire evolution of the body from inception up to treadmilling?

An added complexity of the present problem arises due to the existence of moving boundaries in both the reference and the physical space. Integration of the boundary value problem defined in either (76) or (77), is thus performed via a specialized numerical method that incorporates two integration time scales, to track both the moving boundaries and the diffusion mechanism. In the following, we choose to integrate the boundary value problem in the reference frame to examine the solid matrix and the solvent separately. We solve for $(l^R(t), J(x_1, t))$ in order to describe the time evolution of the system for various initial conditions $(l^R(0), J(x_1, 0))$.

In Fig. 4(a), we plot the evolution of the growing body from an initially homogenous layer of given dry thickness l^R and spatially constant swelling ratio J (indicated by the black dots) towards the treadmilling state (indicated by the blue dot). Given the importance of J_a and its crucial role in driving the coupled growth, results are represented in a phase space defined by the dimensionless dry thickness of the body $l^R(t)/\tilde{l}^R$ and the renormalized swelling ratio $J_a(t)/\tilde{J}_a$. The arrows indicate the direction of the evolution toward treadmilling $(l^R(t)/\tilde{l}^R, J_a(t)/\tilde{J}_a) = (1, 1)$. On this note, it is worth emphasising that the treadmilling limit recovered by space-time integrations agrees with the analytically derived limit in (85).

Two distinct regimes clearly emerge from the evolution paths in Fig. 4(a): first, a *diffusion-dominated regime* during which changes in dry thickness are relatively small, then following a sharp change in trend, a second regime in which surface growth and solvent diffusion are fully coupled. In this regime the system follows a path that is independent of initial conditions and is thus referred to as the *universal path*.

Although only four paths are represented in Fig. 4(a), a comprehensive analysis of the sensitivity to initial conditions (including nonhomogeneous initial states) has been conducted and a similar sharp transition from a diffusion-dominated regime to the universal path has been observed in all cases and across a range of constitutive parameters (Fig. 4(b) shows the universal path for various combinations of ψ_a and λ_0). Nonetheless we identify four different regions in the phase diagram (as indicated by the roman numerals) that are characterized by distinct evolution scenarios. To explain these differences we present in Fig. 4(c) the time dependent evolution of the layers corresponding to the paths represented in Fig. 4(a), each of which initiates in a different region. The physical state of the system at various times is shown via a series of vertical bars that indicate the physical thickness $l(t)$ and with color variation representing the swelling ratio throughout the thickness $J(y_1, t)$. The response in each of the two regime occurs at a different time-scale, hence results are represented first with time scale τ_1 of the diffusion-dominated regime, then with time scale τ_2 of the evolution along the universal path. As previously mentioned, due to the highly nonlinear nature of the considered growth problem, these time scales are dependent on both the model parameters and initial conditions, and are not amenable to simple scaling arguments. To clearly present the results in the different regimes we thus normalize the time with respect to the representative values $\tau_1 = 8.2 \times 10^3$ s and $\tau_2 = 1.6 \times 10^7$ s. Examining Fig. 4(c), we observe non-monotonic evolution of the physical thickness of the body. Layers that initiate in regions I and III are over swollen, and thus release solvent during the diffusion-dominated regime, while those that initiate in regions II and IV are under swollen, and thus intake

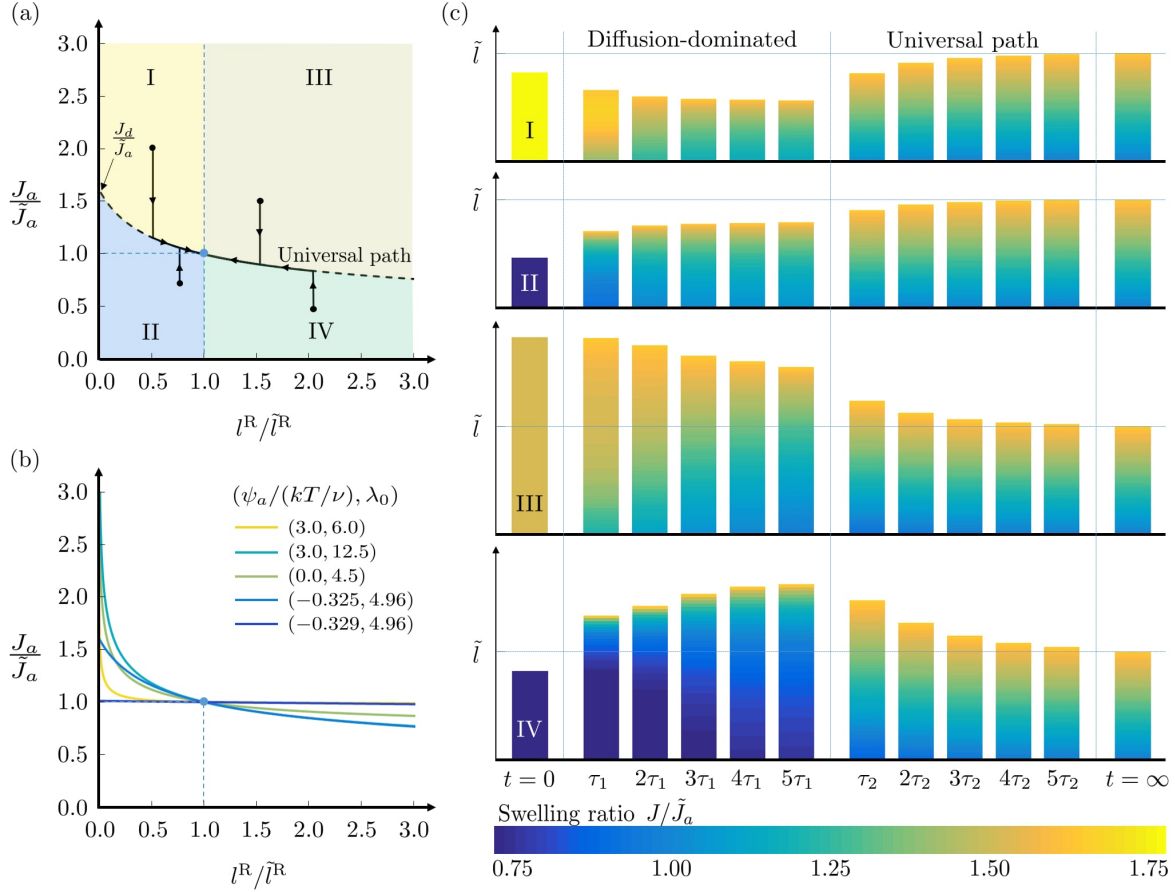


Figure 4: (a) Evolution of a growing system represented in the phase space of normalized association swelling ratio versus normalized dry thickness, with $\psi_a/(kT/\nu) = -0.325$ and $\lambda_0 = 4.96$. Four regions (I - IV) represent different regimes of growth response. A growth path initiating from each region is shown by the black lines with the arrows representing the direction of the evolution. (b) Effect of ψ_a and λ_0 on the universal path represented in the normalized phase space. The universal paths presented in (a) and (b) derived from numerical simulations and analytical formula (89), and are indistinguishable. (c) Time evolution of total thickness in the physical space and swelling ratio throughout the thickness for the specific paths starting in regions I, II, III and IV.

solvent. Once the system has reached the universal path, growth is driven by the coupling between surface growth and diffusion while swelling profiles maintain a nearly self-similar distribution that moves due to the local mechanisms on the boundaries. In this regime changes in dry thickness become significant and occur over a larger time scale. Systems initiating in regions I and II are under grown, and thus undergo an addition of solid mass during evolution along the universal path, while those initiating in region III and IV are over grown, and thus undergo removal of solid mass.

With the identification of the two distinct regimes, based on the numerical analysis, we now return to the analytical formulations to further characterize them by considering the dominant mechanisms that drive each of them.

Diffusion-dominated regime. In this regime, the body undergoes rapid variations in swelling to adjust to its environment, while changes in dry thickness (i.e. surface growth) is insignificant, as shown in Fig. 4(a). The bulk diffusion represented by the differential equation in (77) is thus dominant and defines the time scale of evolution while the time-dependent boundary conditions do not play a significant role, thus explaining the surprisingly straight vertical lines that characterize the diffusion dominated regime in the phase space. The time scale τ_1 associated with this phase is thus proportional to $L^2/(DN\nu)$, where L is a characteristic dry length scale of the system.

Fig. 5 shows the evolution of the swelling ratio during the diffusion-dominated regime for the four paths presented in Fig. 4(a). In all cases, the swelling ratio at the association boundary tends to a nearly asymptotic value as the system transitions to the universal path.

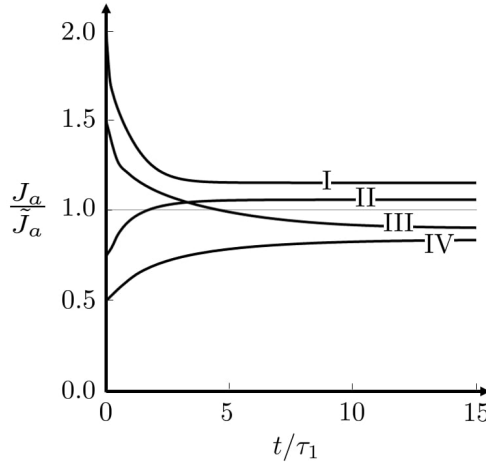


Figure 5: Time evolution of the normalized swelling ratio at the association boundary, during the diffusion-dominated regime for the paths initiating in regions I-IV and presented in Fig. 4(a). Time is normalized by $\tau_1 = 8.2 \times 10^3$ s.

The universal path. After the transient variations of swelling in the diffusion-dominated regime, the system arrives at a quasi-equilibrated state (Fig. 5) in which surface growth and diffusion act harmoniously. This coupled growth is governed by longer time scales hence the time derivative on the left hand side of (76) becomes negligible, while the coupling between diffusion and surface growth is manifested by the boundary condition of (76). The system hence simplifies to

$$\Lambda(J) \frac{dJ}{dy_1} = \frac{V_a^R(J_a)}{\lambda_0^2}. \quad (86)$$

Notice that this relation is similar to the expression for the treadmilling regime (80) with a different that the association rate, and thus varies with time as J_a evolves. In a similar manner to the approach adopted for the treadmilling response, integration of (86) yields an implicit relation between the swelling ratio J and the spatial coordinate y_1

$$y_1(J) = \frac{\lambda_0^2}{V_a^R(J_a)} \int_{J_a}^J \Lambda(J) dJ, \quad (87)$$

and the thickness in the physical space can thus be derived as $\tilde{l} = y_1(J_d)$. By integration of the transformation (57), and substituting equation (86), the distance from the association surface in the reference frame reads

$$\Delta x_1(J) = \frac{\lambda_0^4}{V_a^R(J_a)} \int_{J_a}^J \frac{\Lambda(J)}{J} dJ. \quad (88)$$

Notice that functions $y_1(J)$ and $\Delta x_1(J)$ derived in the above equations are the same as the ones obtained in (81) and (84), with the difference that the swelling ratio has the superscript $(\tilde{\cdot})$ for the treadmilling regime. Analytical expressions of the implicit spatial distribution of swelling are given in equations (B4) and (B5) of Appendix B.

Finally, during the evolution along the universal path, the dry thickness l^R is given by

$$l^R(J_a) = \frac{\lambda_0^4}{V_a^R(J_a)} \int_{J_a}^{J_d} \frac{\Lambda(J)}{J} dJ. \quad (89)$$

This relation between l^R and J_a provides an analytical form for the universal path shown in Figs. 4(a,b). By comparing with numerical results for various initial conditions we find that this analytical form agrees with the numerically derived universal path.

Since the variation of dry thickness (l^R) is insignificant during the diffusion-dominated regime, the initial value of $J_a(0)$ along the universal path (which is the asymptotic value of the diffusion-dominated regime) can be determined by the above equation such that $l^R(J_a(0)) = l_i^R$ where we have reset time to $t = 0$ for the evaluation of the universal path.

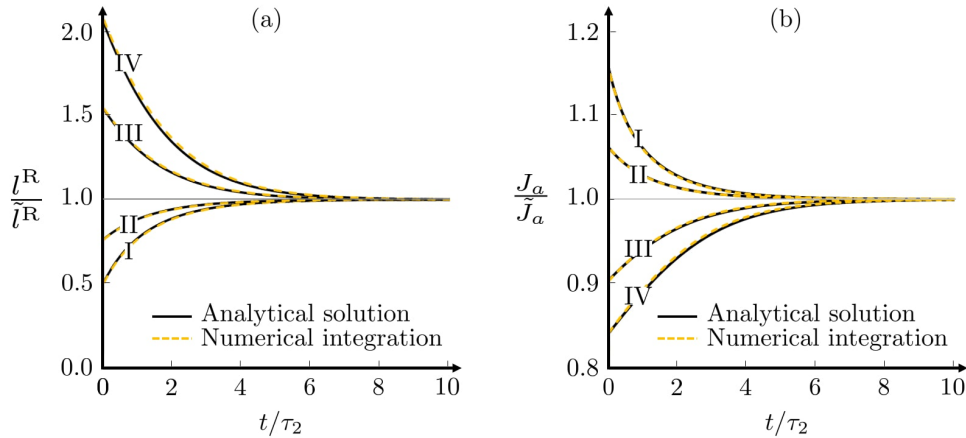


Figure 6: Time evolution of (a) the normalized dry thickness and (b) the normalized swelling ratio at the association boundary along the universal path for initial conditions in regions I-IV presented in Fig. 4(a). Notice that here, $t = 0$ corresponds to time at which evolution along the universal path begins.

The rate of change of the thickness can be determined by differentiating the above equation. Then, comparing the differentiation result with (61) we arrive at a differential equation for $J_a = J_a(t)$, which by integration, reads

$$t = - \int_{J_a(0)}^{J_a(t)} \frac{F(J)}{V_a^R(J) + V_d^R} dJ \quad \text{where} \quad F(J) = \left(\frac{l^R(J)}{V_a^R(J)} \right) \frac{dV_a^R}{dJ} + \frac{\lambda_0^4 \Lambda(J)}{J V_a^R(J)}. \quad (90)$$

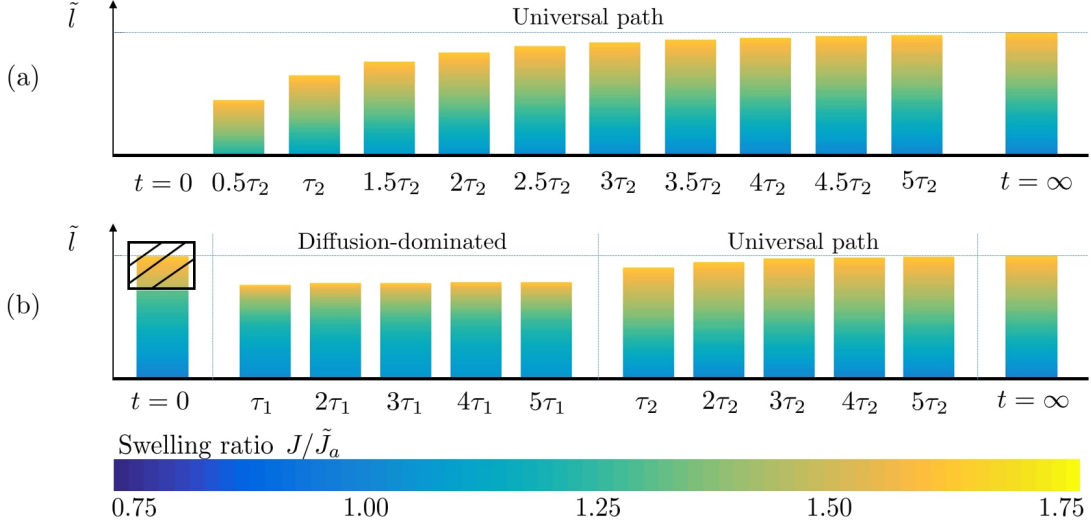


Figure 7: Time evolution of total thickness in the physical space and swelling ratio throughout the thickness for (a) growth starting from inception (b) a perturbed layer by the removal of a piece from the treadmilling regime, with $\psi_a/(kT/\nu) = -0.325$ and $\lambda_0 = 4.96$.

Once $J_a(t)$ is known, the variation of dry thickness is obtained by integration of equation (61) to write

$$l^R(t) = l_i^R + \int_{J_u}^{J_a(t)} (V_a^R(J_a) + V_d^R) dJ_a. \quad (91)$$

In Fig. 6 we compare the time integration results of paths I - IV with the time-evolutions given by (90) and (91). As shown in Fig. 6, the integral analytical expressions are in good agreement with the numerical solutions in predicting the evolution of the swelling ratio and dry thickness evolution.

Body inception and response to perturbation. In all the cases presented, growth has been studied with prescribed initial conditions. A specific challenge arises in defining initial conditions in absence of solid material at the initiation of growth. Inception of a new body, starting from the creation of the very first layer, ensues singularity, since at the time of initiation the association and dissociation surfaces overlap. Nonetheless, it is possible to take advantage of the universal path and to predict the growth of infinitesimally thin layers in the limit $l_i^R \rightarrow 0$. Employing the analytical solutions (90) and (87) to predict the thickness of the body and the swelling ratio throughout the thickness at a given time, we show on Fig. 7(a), the time evolution of a body from an initially nascent state. The evolution then follows the universal path.

Moreover, our solutions suggest that if a perturbation occurs at any time during the evolution, the system will rapidly recover the universal path through a diffusion-dominated regime. Specifically, we show in Fig. 7(b) the response to the perturbation of a treadmilling layer by removal of a portion of its thickness. It is observed that the perturbed body evolves back to treadmilling, after a transitory diffusion-dominated regime of time scale τ_1 followed

by evolution along the universal path of time scale τ_2 . Therefore, the treadmilling regime is the ultimate state towards which the system evolves naturally by following the universal path.

7. Conclusions

A general theoretical framework for kinetics of surface growth coupled with solvent diffusion is presented. To account for conservation of mass in an open system, we consider the formation of a body that is composed of two species (i.e. an elastic matrix and a permeating solvent) and allow for association or dissociation of solvent units on its boundaries. An approach to determine the global natural reference configuration of the growing body in an arbitrary geometry is presented and utilized to determine the driving force of growth. Based on the dissipation inequality, restrictions on the kinetic law that relates between the growth rate and the driving force are defined. As an illustration, the general framework is specialized to consider growth of polymer gels in a uniaxial setting. Numerical integration reveals that following a transient diffusion dominated response, the evolution of a body rapidly tends to a universal path, that is independent of initial conditions, and ultimately leads the system towards a treadmilling state. Any perturbation from the universal path is rapidly recovered, as swelling is adjusted throughout the body and the harmony between the two coupled mechanisms (i.e. growth and diffusion) is restored. The extension of our results to the limit in which the body is an infinitesimally thin layer yields an analytical prediction of the complete evolution of a body, from inception to treadmilling. There remains the philosophical question around the creation of the very first solid layer at the birth of the body, which is beyond the scope of the current framework. Finally, the universal path, that is derived here for a simple geometry, will be at the center of future investigations, which will facilitate this framework to explore more complex geometries. Experimental work will also be key to further illustrate this growth theory and to observe growth along the universal path in a laboratory setting.

Appendix A - Nomenclature

General framework:

\mathcal{R}	body manifold in the physical configuration
\mathcal{R}^R	material manifold in the reference configuration
$\partial\mathcal{R}$	surface boundary of \mathcal{R}
$\partial\mathcal{R}^R$	surface boundary of \mathcal{R}^R
\mathcal{S}_a	association surface in the physical configuration
\mathcal{S}_a^R	association surface in the reference configuration
\mathcal{S}_d	dissociation surface in the physical configuration
\mathcal{S}_d^R	dissociation surface in the reference configuration
t	time variable
\mathbf{y}	spatial point in the physical configuration
\mathbf{x}	material point in the reference configuration
$\hat{\mathbf{y}}$	one on one mapping from reference configuration to physical configuration
$\hat{\mathbf{x}}$	inverse one on one mapping from physical configuration to reference configuration
\mathbf{n}	outward pointing normal vector on the boundary $\partial\mathcal{R}$ in the physical configuration
\mathbf{n}^R	outward pointing normal vector on the boundary
$\partial\mathcal{R}^R$	in the reference configuration
dV_y	volume element in the physical configuration
dV_x	volume element in the reference configuration
dA_y	area element in the physical configuration
dA_x	area element in the reference configuration
\mathbf{v}	particle velocity in the physical configuration
\mathbf{V}	boundary velocity in the physical configuration
\mathbf{V}_G	growth velocity in the physical configuration
\mathbf{V}^R	boundary velocity in the reference configuration
\mathbf{j}	flux of solvent in the physical configuration
\mathbf{j}^R	flux of solvent in the reference configuration
\mathbf{F}	deformation gradient
J	volume ratio
ϕ	physical volume fraction of solvent in the body
ϕ^R	referential volume fraction of solvent in the body
ψ	Helmholtz free energy of the body
ψ_e	Helmholtz elastic free energy associated with the solid matrix
ψ_s	Helmholtz free energy of the solvent
\mathbf{T}	Cauchy stress tensor
\mathbf{S}	Piola stress tensor
\mathbf{b}	body forces in the physical configuration
\mathbf{b}^R	body forces in the reference configuration
p	hydrostatic pressure
μ	chemical potential of the solvent
f	driving force on the boundary
$\Delta\psi$	latent energy of growth
\mathcal{G}	growth function

Specific problem:

k	Boltzmann constant
T	temperature
N	number of polymer chains per unit volume
ν	volume of a solvent unit
χ	Flory-Huggins interaction parameter
D	diffusion coefficient
b	reaction constant
ψ_0	free energy of the unmixed solvent
ψ_a	potential energy gain at the association boundary
λ_0	imposed in-plane stretch

Appendix B - Explicit Formula

In the following, we provide the full analytical formula that have been represented in condensed form in the main text.

The continuity of the chemical potential (72) is

$$\ln \left(1 - \frac{1}{J_d} \right) + \frac{1}{J_d} + \frac{\chi}{J_d^2} + N\nu \left(\frac{J_d}{\lambda_0^4} - \frac{1}{J_d} \right) = 0. \quad (\text{B1})$$

Equation (69) that relates the driving force to the swelling ratio can be further developed using (42)-(44), (49), (50) and (67) to write the driving force at the association boundary as

$$\begin{aligned} f_a(J_a) = \psi_0 + \psi_a - \frac{kT}{\nu} (J_a - 1) \left[\ln \left(1 - \frac{1}{J_a} \right) + \frac{\chi}{J_a} \right] - \frac{NkT}{2} \left(\frac{J_a^2}{\lambda_0^4} + 2\lambda_0^2 - 3 - 2 \ln J_a \right) \\ + \left\{ \frac{kT}{\nu} \left[\ln \left(1 - \frac{1}{J_a} \right) + \frac{1}{J_a} + \frac{\chi}{J_a^2} \right] + NkT \left(\frac{J_a}{\lambda_0^4} - \frac{1}{J_a} \right) \right\} J_a, \end{aligned} \quad (\text{B2})$$

and at the dissociation boundary as

$$f_d(J_d) = \psi_0 (1 + J_d) - \frac{kT}{\nu} (J_d - 1) \left[\ln \left(1 - \frac{1}{J_d} \right) + \frac{\chi}{J_d} \right] - \frac{NkT}{2} \left(\frac{J_d^2}{\lambda_0^4} + 2\lambda_0^2 - 3 - 2 \ln J_d \right). \quad (\text{B3})$$

Substituting (51) and (71) in (87) and (88), we can write in the physical space

$$\begin{aligned} y_1(J) = \frac{\lambda_0^2 D}{b \sinh \left(\frac{\nu}{kT} f_a(J_a) \right)} \left\{ \frac{N\nu}{\lambda_0^4} \left[\ln \left(\frac{J}{J_a} \right) + \frac{1}{J} - \frac{1}{J_a} \right] - \frac{N\nu}{2} \left(\frac{1}{J^2} - \frac{1}{J_a^2} \right) + \right. \\ \left. \frac{1}{3} (N\nu + 2\chi - 1) \left(\frac{1}{J^3} - \frac{1}{J_a^3} \right) - \frac{\chi}{2} \left(\frac{1}{J^4} - \frac{1}{J_a^4} \right) \right\}, \end{aligned} \quad (\text{B4})$$

and in the reference space

$$\Delta x_1(J) = \frac{\lambda_0^4 D}{b \sinh\left(\frac{\nu}{kT} f_a(J_a)\right)} \left[\frac{N\nu}{\lambda_0^4} \left(-\frac{1}{J} + \frac{1}{J_a} + \frac{1}{2J^2} - \frac{1}{2J_a^2} \right) - \frac{N\nu}{3} \left(\frac{1}{J^3} - \frac{1}{J_a^3} \right) + \right. \\ \left. \frac{1}{4} (N\nu + 2\chi - 1) \left(\frac{1}{J^4} - \frac{1}{J_a^4} \right) - \frac{2\chi}{5} \left(\frac{1}{J^5} - \frac{1}{J_a^5} \right) \right]. \quad (\text{B5})$$

Analytical expressions for (81) and (84) can be obtained by replacing J and J_a in (B4) and (B5) by \tilde{J} and \tilde{J}_a . Notice that the determination of J_a is required to use the above relations: during the evolution along the universal path, the swelling ratio at the association boundary $J_a(t)$ can be determined at any time using implicit equation (90); for the treadmilling regime, the swelling ratio at the association boundary \tilde{J}_a is implicitly determined using the balance between addition and removal of mass (79) combined combination with the kinetic law (51), and satisfies

$$f_a(\tilde{J}_a) = -f_d(J_d). \quad (\text{B6})$$

The thickness of the material, in both the physical and the reference frames, l and l^R , is obtained by taking the values of (B4) and (B5) respectively, for $J = J_d$.

References

- Ambrosi, D., Ateshian, G., Arruda, E., Cowin, S., Dumais, J., Goriely, A., Holzapfel, G. A., Humphrey, J., Kemkemer, R., Kuhl, E., et al., 2011. Perspectives on biological growth and remodeling. *Journal of the Mechanics and Physics of Solids* 59 (4), 863–883.
- Ambrosi, D., Mollica, F., 2002. On the mechanics of a growing tumor. *International journal of engineering science* 40 (12), 1297–1316.
- Ambrosi, D., Preziosi, L., 2009. Cell adhesion mechanisms and stress relaxation in the mechanics of tumours. *Biomechanics and modeling in mechanobiology* 8 (5), 397–413.
- Archer, R. R., 2013. Growth stresses and strains in trees. Vol. 3. Springer Science & Business Media.
- Ateshian, G. A., 2007. On the theory of reactive mixtures for modeling biological growth. *Biomechanics and modeling in mechanobiology* 6 (6), 423–445.
- Bauër, P., Tavecchi, J., Pujol, T., Planade, J., Heuvingh, J., Du Roure, O., 2017. A new method to measure mechanics and dynamic assembly of branched actin networks. *Scientific reports* 7, 15688.
- Bauhofer, A., Krödel, S., Bilal, O., Daraio, C., Constantinescu, A., 2017. Direct laser writing of single-material sheets with programmable self-rolling capability. *Bulletin of the American Physical Society* 62.

- Ben Amar, M., Ciarletta, P., 2010. Swelling instability of surface-attached gels as a model of soft tissue growth under geometric constraints. *Journal of the Mechanics and Physics of Solids* 58 (7), 935–954.
- Ben Amar, M., Goriely, A., 2005. Growth and instability in elastic tissues. *Journal of the Mechanics and Physics of Solids* 53 (10), 2284–2319.
- Chester, S. A., Anand, L., 2010. A coupled theory of fluid permeation and large deformations for elastomeric materials. *Journal of the Mechanics and Physics of Solids* 58 (11), 1879–1906.
- Ciarletta, P., Preziosi, L., Maugin, G., 2013. Mechanobiology of interfacial growth. *Journal of the Mechanics and Physics of Solids* 61 (3), 852–872.
- Correa, D., Papadopoulou, A., Guberan, C., Jhaveri, N., Reichert, S., Menges, A., Tibbits, S., 2015. 3d-printed wood: Programming hygroscopic material transformations. *3D Printing and Additive Manufacturing* 2 (3), 106–116.
- Cyron, C., Humphrey, J., 2017. Growth and remodeling of load-bearing biological soft tissues. *Meccanica* 52 (3), 645–664.
- Dervaux, J., Ben Amar, M., 2011. Buckling condensation in constrained growth. *Journal of the Mechanics and Physics of Solids* 59 (3), 538–560.
- DiCarlo, A., 2005. Surface and bulk growth unified. In: *Mechanics of material forces*. Springer, pp. 53–64.
- Duda, F. P., Souza, A. C., Fried, E., 2010. A theory for species migration in a finitely strained solid with application to polymer network swelling. *Journal of the Mechanics and Physics of Solids* 58 (4), 515–529.
- Feynman, R. P., Leighton, R. B., Sands, M., 1963. *The Feynman Lectures on Physics*. Vol. 1. Elsevier.
- Flory, P. J., 1942. Thermodynamics of high polymer solutions. *The Journal of chemical physics* 10 (1), 51–61.
- Flory, P. J., Rehner, J. J., 1943. Statistical mechanics of cross-linked polymer networks ii. swelling. *The Journal of Chemical Physics* 11 (11), 521–526.
- Fried, E., Gurtin, M. E., 2004. A unified treatment of evolving interfaces accounting for small deformations and atomic transport with emphasis on grain-boundaries and epitaxy. *Advances in applied mechanics* 40, 1–177.
- Ganghoffer, J.-F., Goda, I., 2018. A combined accretion and surface growth model in the framework of irreversible thermodynamics. *International Journal of Engineering Science* 127, 53–79.
- Gibson, I., Rosen, D., Stucker, B., 2014. *Additive manufacturing technologies: 3D printing, rapid prototyping, and direct digital manufacturing*. Springer.

- Goriely, A., 2017. The mathematics and mechanics of biological growth. Vol. 45. Springer.
- Gurtin, M. E., 2008. Configurational forces as basic concepts of continuum physics. Vol. 137. Springer Science & Business Media.
- Holland, M. A., Kosmata, T., Goriely, A., Kuhl, E., 2013. On the mechanics of thin films and growing surfaces. *Mathematics and Mechanics of Solids* 18 (6), 561–575.
- Hong, W., Zhao, X., Zhou, J., Suo, Z., 2008. A theory of coupled diffusion and large deformation in polymeric gels. *Journal of the Mechanics and Physics of Solids* 56 (5), 1779–1793.
- Humphrey, J. D., Dufresne, E. R., Schwartz, M. A., 2014. Mechanotransduction and extracellular matrix homeostasis. *Nature reviews Molecular cell biology* 15 (12), 802–812.
- Kaur, I., Pandya, D., Chopra, K., 1980. Growth kinetics and polymorphism of chemically deposited cds films. *Journal of the Electrochemical Society* 127 (4), 943–948.
- Kim, D.-H., Jang, H.-S., Kim, C.-D., Cho, D.-S., Yang, H.-S., Kang, H.-D., Min, B.-K., Lee, H.-R., 2003. Dynamic growth rate behavior of a carbon nanotube forest characterized by in situ optical growth monitoring. *Nano Letters* 3 (6), 863–865.
- Loeffel, K., Anand, L., 2011. A chemo-thermo-mechanically coupled theory for elastic-viscoplastic deformation, diffusion, and volumetric swelling due to a chemical reaction. *International Journal of Plasticity* 27 (9), 1409–1431.
- Louchev, O. A., Laude, T., Sato, Y., Kanda, H., 2003. Diffusion-controlled kinetics of carbon nanotube forest growth by chemical vapor deposition. *The Journal of chemical physics* 118 (16), 7622–7634.
- Mane, R., Lokhande, C., 2000. Chemical deposition method for metal chalcogenide thin films. *Materials Chemistry and Physics* 65 (1), 1–31.
- Mattevi, C., Kim, H., Chhowalla, M., 2011. A review of chemical vapour deposition of graphene on copper. *Journal of Materials Chemistry* 21 (10), 3324–3334.
- Menzel, A., Kuhl, E., 2012. Frontiers in growth and remodeling. *Mechanics research communications* 42, 1–14.
- Meyyappan, M., Delzeit, L., Cassell, A., Hash, D., 2003. Carbon nanotube growth by pecvd: a review. *Plasma Sources Science and Technology* 12 (2), 205.
- Mitchison, T., Cramer, L., 1996. Actin-based cell motility and cell locomotion. *Cell* 84 (3), 371–379.
- Mogilner, A., Oster, G., 1996. Cell motility driven by actin polymerization. *Biophysical journal* 71 (6), 3030–3045.
- Mogilner, A., Oster, G., 2003a. Force generation by actin polymerization ii: the elastic ratchet and tethered filaments. *Biophysical journal* 84 (3), 1591–1605.

- Mogilner, A., Oster, G., 2003b. Polymer motors: pushing out the front and pulling up the back. *Current biology* 13 (18), R721–R733.
- Moulton, D. E., Goriely, A., Chirat, R., 2012. Mechanical growth and morphogenesis of seashells. *Journal of theoretical biology* 311, 69–79.
- Nair, M., Nair, P., 1991. Simplified chemical deposition technique for good quality sns thin films. *Semiconductor science and technology* 6 (2), 132.
- Noireaux, V., Golsteyn, R., Friederich, E., Prost, J., Antony, C., Louvard, D., Sykes, C., 2000. Growing an actin gel on spherical surfaces. *Biophysical journal* 78 (3), 1643–1654.
- Papastavrou, A., Steinmann, P., Kuhl, E., 2013. On the mechanics of continua with boundary energies and growing surfaces. *Journal of the Mechanics and Physics of Solids* 61 (6), 1446–1463.
- Skalak, R., Dasgupta, G., Moss, M., Otten, E., Dullemeijer, P., Vilmann, H., 1982. Analytical description of growth. *Journal of Theoretical Biology* 94 (3), 555–577.
- Skalak, R., Farrow, D., Hoger, A., 1997. Kinematics of surface growth. *Journal of mathematical biology* 35 (8), 869–907.
- Sozio, F., Yavari, A., 2017. Nonlinear mechanics of surface growth for cylindrical and spherical elastic bodies. *Journal of the Mechanics and Physics of Solids* 98, 12–48.
- Szost, B. A., Terzi, S., Martina, F., Boisselier, D., Prytuliak, A., Pirling, T., Hofmann, M., Jarvis, D. J., 2016. A comparative study of additive manufacturing techniques: Residual stress and microstructural analysis of clad and waam printed ti-6al-4v components. *Materials & Design* 89, 559–567.
- Tepole, A. B., Ploch, C. J., Wong, J., Gosain, A. K., Kuhl, E., 2011. Growing skin: a computational model for skin expansion in reconstructive surgery. *Journal of the Mechanics and Physics of Solids* 59 (10), 2177–2190.
- Theriot, J. A., 2000. The polymerization motor. *Traffic* 1 (1), 19–28.
- Thompson, D. W., 1970. *On growth and form*, 1917. Cambridge [Eng.]: University press. xv.
- Tomassetti, G., Cohen, T., Abeyaratne, R., 2016. Steady accretion of an elastic body on a hard spherical surface and the notion of a four-dimensional reference space. *Journal of the Mechanics and Physics of Solids* 96, 333–352.
- Treloar, L. R. G., 1975. *The physics of rubber elasticity*. Oxford University Press, USA.
- Zöllner, A. M., Tepole, A. B., Kuhl, E., 2012. On the biomechanics and mechanobiology of growing skin. *Journal of theoretical biology* 297, 166–175.
- Zurlo, G., Truskinovsky, L., 2017. Printing non-euclidean solids. *arXiv preprint arXiv:1703.03082*.